

van der Waals forces in nonrelativistic quark models of the NN interaction

Ralph Girard* and Jean LeTourneux

Laboratoire de Physique Nucléaire, Université de Montréal, Montréal, H3C 3J7, Canada

(Received 17 December 1992; revised manuscript received 1 April 1994)

The van der Waals force induced by color-dependent confining potentials in nonrelativistic quark models of the NN interaction is investigated through a full resonating group calculation where the NN channel is coupled to a channel of two orbitally polarized color octets. While exchange terms can be neglected at low energies, they prove to be essential at higher energies, where the short and intermediate ranges of the induced interaction are probed. The extent to which the latter can be simulated by effective local potentials is examined. Finally, the van der Waals force induced by a strong enough confining potential is shown to give rise to unphysical bound states.

PACS number(s): 12.38.Aw, 12.39.-x, 13.75.Cs

In nonrelativistic quark models of the NN interaction, a long-range van der Waals (vdW) force is induced when the phenomenological confining potential is allowed to admix CC configurations formed of two orbitally excited color octets. For confining potentials in r or r^2 , this force decreases as a low inverse power of the distance and is, therefore, generally considered as a pathological feature of the model. Nevertheless, it has been argued [1] that the NN interaction is free from meson-exchange effects and dominated by residual qq forces at less than about 2 fm, so that the vdW attraction is meaningful and should be retained in that intermediate range, while in a more realistic description it should be damped by $q\bar{q}$ pair creation at larger distances.

Most of the resonating group (RG) calculations so far [2] have shown no manifestation of such a force, since the potentially troublesome configurations were neglected. Whichever point of view one adopts with regard to this force, one should obviously compute its effects properly once at least in order to know exactly what they are. In earlier perturbative calculations [3,4], second-order energy shifts were usually computed as a function of the intercluster distance; since the latter was assumed to be large, exchange effects were neglected and the resulting potential was local; various approximations were made for the energy of the intermediate CC state. Clearly, such a treatment is inadequate: the NN and CC configurations are strongly coupled and should be treated dynamically according to the coupled-channel RG formalism. Moreover, exchange effects should be fully taken into account in order to determine the influence of the polarized CC configuration at short and intermediate ranges, where it may be argued to make physical sense. Maltman and Isgur [1] treated exchange effects properly, but unfortunately did not solve the coupled RG equations, since the configuration responsible for the vdW interactions was introduced perturbatively. Moreover, the wave functions describing the relative motion of the clusters, in their variational calculation, were expressed as finite sums of Gaussians. While this may be a reason-

able description for the CC channel, it is not likely to be so for the NN channel in the presence of an induced long-range force. In their two-channel RG calculation, Pfenninger and Faessler [5] neglected all exchange terms and retained only the confining part of the qq interaction when computing the kernels of the CC channel as well as those connecting the NN and the CC channels. These approximations are not expected to affect significantly the long-range effects of the CC channel, but they are likely to provide an inaccurate description in the short and medium ranges.

This paper presents a full two-channel calculation in the RG formalism. All exchange terms are retained and the full qq Hamiltonian is used throughout the whole calculation. The same channels are taken into account as in Ref. [5]. Thus, the total wave function is

$$\begin{aligned} \Psi_{ST} = \sum_{l_0 l J} \mathcal{A} \{ & [[\chi^N(1, 2, 3)\chi^N(4, 5, 6)]_{l_0 ST} g_N^l(r) Y_l(\hat{\mathbf{r}})]_L \\ & + [[\chi^C(1, 2, 3)\chi^C(4, 5, 6)]_{l_0 ST} \\ & \times g_C^l(r) Y_l(\hat{\mathbf{r}})]_L \} \quad (1) \end{aligned}$$

where \mathcal{A} is the antisymmetrizing operator, while χ^α is the internal wave function for a three-quark cluster in state $\alpha = N$ or C . The relative motion of the clusters is described by the RG amplitude $g_\alpha(\mathbf{r}) \equiv \sum_l g_\alpha^l(r) Y_l(\hat{\mathbf{r}})$, \mathbf{r} being the distance between their centers of mass. The orbital angular momenta, spins, and isospins of the two clusters are coupled to l_0 , S , and T , respectively, l is the relative motion orbital angular momentum, and, finally, $\mathbf{L} = l_0 + l$, and $\mathbf{J} = \mathbf{L} + \mathbf{S}$.

The internal wave function of a nucleon, χ^N , is the product of a symmetric orbital wave function, ψ^0 ($[3]$), an antisymmetric color singlet, ψ^c ($[1^3]$), and a symmetric spin-isospin factor ψ^{st} ($[3]$) formed by combining two [21] representations with $s = \frac{1}{2}$ and $t = \frac{1}{2}$. The symbol $[f]$ denotes the Young symmetry for the group S_3 . When the confining part of the qq interaction is st independent, the two octets of the simplest CC configuration giving rise to a vdW interaction are in the same st state as the nucleon, while the two [21] symmetries of their orbital and color parts are coupled to $[1^3]$. The lowest [21] orbital states are formed by promoting a quark from a $1s$ to a $1p$ orbit. The vanishing orbital angular momenta of the two

*Present address: MPB Technologies Inc., Dorval, H9P 1J1, Canada.

nucleons can only be coupled to $l_0 = 0$ in Eq. (1), while l_0 can take the values 0, 1, or 2 for the two polarized octets in p states. We study the NN system in the $l = 0$ partial wave only and neglect arbitrarily the coupling to other values of l arising in the CC channel for $l_0 \neq 0$. Thus, only the $l_0 = 0$ configuration will be retained in the CC channel. Then, $L = 0$ and $J = S$. Obviously, the six-quark wave function must be a color singlet.

The amplitudes $g_\alpha(\mathbf{r})$ are determined by the set of coupled RG equations

$$\sum_{\beta} \int [H_{\alpha\beta}(\mathbf{r}, \mathbf{r}') - EN_{\alpha\beta}(\mathbf{r}, \mathbf{r}')] g_{\beta}(\mathbf{r}') d\mathbf{r}' = 0, \quad (2)$$

the overlap and energy kernels, $N_{\alpha\beta}(\mathbf{r}, \mathbf{r}')$ and $H_{\alpha\beta}(\mathbf{r}, \mathbf{r}')$,

$$\left[-\frac{\hbar^2}{2\mu} \left(\frac{d^2}{dr^2} - \frac{l(l+1)}{r^2} \right) - E_{c.m.} \right] u_{\alpha}^l(r) + \sum_{\beta=N,C} \left[U_{\alpha\beta}^l(r) u_{\beta}^l(r) + \int_0^{\infty} K_{N\beta}^l(r, r') u_{\beta}^l(r') dr' \right] = 0, \quad (4)$$

where $u_{\alpha}^l \equiv r g_{\alpha}^l(r)$ and the channel indices N and C stand for NN and CC , respectively. The reduced mass μ is $3m_q/2$ and $E_{c.m.} \equiv (\hbar^2/2\mu)k^2 + 2E_N$ is the total energy in the center of mass system, k being the relative momentum in the NN channel and E_N the internal energy of a N cluster. Finally, $U_{\alpha\beta}^l$ and $K_{\alpha\beta}^l$ are the projections on the l th partial wave of the local potential part of $H_{\alpha\beta}(\mathbf{r})$ and of the nonlocal part of $H_{\alpha\beta} - E_{c.m.}N_{\alpha\beta}$, respectively.

We solved these equations by discretizing them at N points over a finite range $0 \leq r \leq r_{\max}$ and imposing an appropriate boundary condition at $r = r_{\max}$. The nucleons are not free asymptotically, but subjected to the attractive tail of the vdW potential, which behaves like $-c/r^2$, as shown below [Eq. (8)]. The interior solution $u_N(r)$ should therefore be matched with a linear combination of two independent positive energy solutions $F_l(r)$ and $G_l(r)$ of the Schrödinger equation with $V = -c/r^2$. The value of the parameter $K_l \equiv 2\mu c / [\hbar(l + \frac{1}{2})]^2$ determines which pair of solutions should be used. For $K_l < 1$, F_l and G_l involve $J_{\nu}(kr)$ and $N_{\nu}(kr)$ with $\nu = (l + \frac{1}{2})\sqrt{1 - K_l}$, while for $K_l > 1$, ν becomes imaginary and it proves convenient to work with the real and imaginary parts of J_{ν} in order to keep the system of equations real. Since all these Bessel functions tend towards sines and cosines in the extreme asymptotic region, phase shifts can be extracted easily [7]. Although for r_{\max} large enough these trigonometric limits can be used directly in the matching condition, it is highly advisable not to do so if r_{\max} is to be kept as low as a few fm, so as to have shorter computation times and greater numerical stability.

Potentials 1.a and 1.d of Ref. [6] were used in the calculations, with $m_q = 362$ MeV. They were chosen because they yield values for c (53.8 and 8.1 MeV fm²) and K_l (6.0 and 0.90) that lead to different matching conditions. The $(S, T) = (1, 0)$ phase shifts as calculated with these two potentials are presented in Figs. 1 and 2. Results for the $(S, T) = (0, 1)$ case are quite similar and are therefore not presented.

being defined in the usual way. For the sake of computational convenience, the phenomenological qq interaction of Ref. [6] was used,

$$V_{ij} = \frac{\lambda_i}{2} \cdot \frac{\lambda_j}{2} [Br_{ij}^2 + Ae^{-r_{ij}^2/\alpha^2} + C + D\boldsymbol{\sigma}_i \cdot \boldsymbol{\sigma}_j \delta(\mathbf{r}_i - \mathbf{r}_j)]. \quad (3)$$

A very elaborate code was written in MACSYMA (see Ref. [7] for details), which computed completely all the RG kernels, projected them on the $l = 0$ partial wave, and, finally, transferred the resulting analytical expressions directly to the code solving the system of integro-differential equations. After projection, the latter became

Potential 1.a induces a much stronger vdW interaction than potential 1.d. This is easily understood by looking at the asymptotic behavior of the induced potential given below [Eq. (7)]. Besides the fact that the first potential has a larger confining part than the second one ($B = -621$ and -215 MeV fm⁻², respectively), the difference $E_C - E_N$ between the masses of the C and N clusters is smaller for potential 1.a (785 MeV) than for potential 1.d (1151 MeV). Long-range effects of the vdW interaction are particularly important at low energies, where the short-range contribution coming from the exchange terms is not probed. They are therefore well reproduced, at such energies, by a truncated two-channel calculation in which all exchange terms are dropped. At higher energies, however, the truncated calculation is seen to exaggerate the effect of the CC channel, and a full calculation has to be performed in order to describe correctly all the effects of this channel, and not only the vdW interaction it induces.

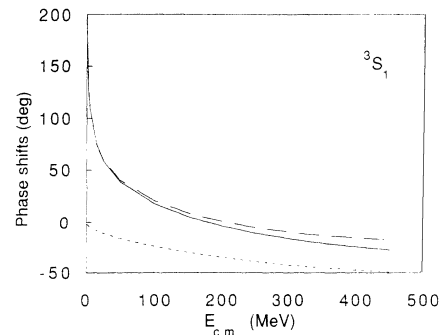


FIG. 1. Phase shifts for S-wave scattering in the $(S, T) = (1, 0)$ channel, as calculated with potential 1.a of Ref. [6]. The solid line corresponds to the full two-channel calculation, the short-dashed line to the one-channel calculation, and the long-dashed line to a truncated two-channel calculation where the exchange terms (including the local ones coming from the δ -function part of the potential) were dropped everywhere except in the NN channel.

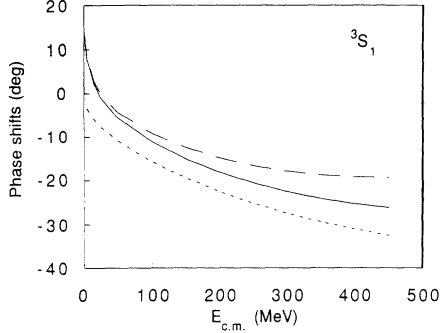


FIG. 2. Same as Fig. 1, but for potential 1.d of Ref. [6].

Most of the earlier discussions of the long-range induced vdW interaction were formulated in terms of effective local potentials. It may be interesting, therefore, to compare our results with those yielded by such an approach. Of course, there is no unique prescription for constructing an effective potential. What will be done here is quite close to the spirit of earlier work, where, essentially, second-order perturbation theory was used, or an approximate effective potential like that of Feshbach [8] was derived. In order to extract an approximate local potential from Eqs. (4), one should first drop the non-local kernels K_{NC}^l, K_{CN}^l , and K_{CC}^l . The kernel K_{NN}^l will be kept, though, so as to exhibit how an effective potential taking implicitly the CC channel into account modifies the initial one-channel scattering problem. The local exchange terms coming from the δ -function part of the potential will be dropped in the CN , NC , and CC kernels. Since the terms we neglect are short ranged, the tail of the effective interaction is not affected by this approximation. The only source of nonlocality that is left appears upon elimination of the CC channel, as a consequence of its kinetic energy operator. Dropping the latter from Eq. (4) for the CC channel, on the ground that it is likely to be relatively small as compared with the confining potential at large distances, one gets, for the $l = 0$ partial wave, after elimination of the amplitude $u_C(r)$,

$$\left[-\frac{\hbar^2}{2\mu} \frac{d^2}{dr^2} + U_{NN}^0(r) + V^{\text{eff}}(r) - E_{\text{c.m.}} \right] u_N(r) + \int dr' K_{NN}^0(r, r') u_N(r') = 0, \quad (5)$$

where

$$V^{\text{eff}}(r) \equiv \frac{|U_{NC}^0(r)|^2}{\hbar^2 k^2 / 2\mu + 2E_N - U_{CC}^0(r)}. \quad (6)$$

Beside making V^{eff} energy dependent, the k^2 term in the denominator can, when sufficiently large, cancel the other two terms, thus yielding, for decreasing r , a very strong short-range attraction followed by a strong repulsion of even shorter range. Phase shifts computed with such a V^{eff} are completely pathological, and, since this problem is not unrelated with our neglect of the kinetic energy operator in the CC channel, the term $\hbar^2 k^2 / 2\mu$ in

(6) will equally be dropped. We will call V_a^{eff} the potential thus obtained, with the full expressions for U_{NC}^0 and U_{CC}^0 . Further simplification is achieved when the latter are replaced by their asymptotic limits, namely, $\sqrt{6}Bb^2$ for $U_{NC}^0(r)$ and $2E_C - 3C - 3B(3b^2 + r^2)$ for $U_{CC}^0(r)$. This yields the asymptotic effective potential

$$V_b^{\text{eff}}(r) = \frac{6B^2b^4}{2(E_N - E_C) + 3C + 3B(3b^2 + r^2)}. \quad (7)$$

In the extreme asymptotic limit, the r^2 term dominates in U_{CC} , and V_b^{eff} reduces to

$$V_c^{\text{eff}}(r) = \frac{2Bb^4}{r^2} \equiv -\frac{c}{r^2}, \quad (8)$$

which agrees with the expression derived by the Orsay group [3],

$$V_{\text{Ors}}^{\text{eff}}(r) = -\frac{2}{3}a\alpha^2(\alpha^2 - 2\alpha + 3)\langle r_1^2 \rangle^2 r^{\alpha-4}, \quad (9)$$

for the van der Waals interaction induced by a confining qq potential $V_{ij}^{(c)} = -a\lambda_i \cdot \lambda_j r_{ij}^\alpha$. In Eq. (9), $\langle r_1^2 \rangle$ is the mean value of r_1^2 in a nucleon, \mathbf{r}_1 being the position of any quark relative to the center of mass of the nucleon. With our orbital wave function ψ^0 ([3]), $\langle r_1^2 \rangle = b^2$.

In Fig. 3, the phase shifts of the full two-channel calculation are compared with those obtained from Eq. (5) when V^{eff} is replaced by V_a^{eff} , V_b^{eff} , or $V_{\text{Ors}}^{\text{eff}}$. Up to relative energies of the order of 100 MeV, V_a^{eff} and V_b^{eff} reproduce the phase shifts of the full calculation within less than 4° . As the energy increases, they yield essentially identical results, which overestimate more and more the attraction induced by the CC channel. The simplest of the effective potentials, $V_{\text{Ors}}^{\text{eff}}$, is seen to overestimate this attraction considerably at all energies. The relative degree of accuracy that can be achieved with the various effective potentials seems to depend strongly on the choice of the qq interaction, as can be seen from Fig. 4, which shows

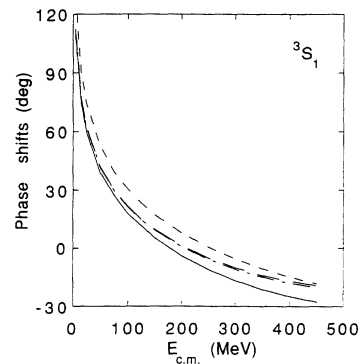


FIG. 3. Comparison between the phase shifts obtained in the full two-channel calculation and in the one-channel approximation, Eq. (5), with an effective potential. These phase shifts were computed with the qq interaction 1.a of Ref. [6] in the $(S, T) = (1, 0)$ channel. The solid line corresponds to the full two-channel calculation, while the dot-dashed, long-dashed, and short-dashed curves correspond to the one-channel calculations performed with V_a^{eff} , V_b^{eff} , and $V_{\text{Ors}}^{\text{eff}}$, respectively.

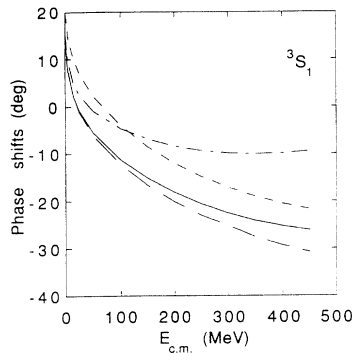


FIG. 4. Same as Fig. 3, but for potential 1.d of Ref. [6].

the same quantities as Fig. 3, but for the interaction 1.d. While $V_{\text{Ors}}^{\text{eff}}$ is still too attractive at all energies, V_a^{eff} and V_b^{eff} now yield very different results, because V_a^{eff} develops at short range a strong attraction that does even overtake momentarily that of $V_{\text{Ors}}^{\text{eff}}$, as a consequence of the short-range terms in the numerator of (6). Thus V_a^{eff} provides the least reliable approximation for this qq interaction. One should therefore not expect V_a^{eff} to be necessarily a better approximation than V_b^{eff} , just because it retains some of the short-ranged terms: comparable or even larger terms may have been dropped.

Asymptotically, Eq. (5) reduces to a Schrödinger equation with an r^{-2} potential. Then, the number of bound solutions is finite or infinite [9] according as K_l is smaller or larger than 1. Since both situations are realized in the $l = 0$ partial wave with the two qq potentials we use, for one at least of them our system must have some bound states. In order to look for the latter, Eqs. (4) were discretized, second derivatives being approximated through second central differences. The resulting eigenvalue problem was not a standard one, because of the overlap kernel that multiplies E . This was remedied in the usual fashion, by multiplying all kernels from the left and from the right by the square root of the inverse of the

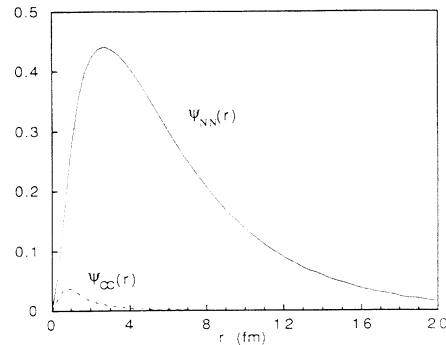


FIG. 5. NN and CC components of the wave function of the bound state occurring at -2.0 MeV in the $(S, T) = (1, 0)$ channel for potential 1.a of Ref. [6].

overlap kernel. The resulting matrix was diagonalized in the $(S, T) = (1, 0)$ channel for potentials 1.a and 1.d. Because of the long range of the induced vdW interaction, we had to ascertain that the diagonalization was carried out with a sufficiently large value of r_{max} . No bound state was found for potential 1.d, but one was easily obtained for the other potential, at an energy $E = -2.0$ MeV, which became essentially stable for $r_{\text{max}} > 50$ fm. Its wave function is shown in Fig. 5. Quite obviously, this bound state is completely pathological and should in no way be considered as approximating the deuteron bound state. As the value of r_{max} was further increased, the lowest positive energy states kept moving steadily towards zero, and it seems quite likely that more and more bound states would have appeared had the calculation been performed for $r_{\text{max}} \gg 100$ fm. However, this somewhat academic investigation was not pursued any further, in view of the computer time involved.

One of us (J.L.) thanks J.-M. Lina and M. Mayrand for computational advice. This work was supported in part by NSERC of Canada and the Fonds FCAR of Québec.

- [1] K. Maltman and N. Isgur, Phys. Rev. D **29**, 952 (1984).
- [2] For a review, see, for instance, F. Myrher, Rev. Mod. Phys. **60**, 629 (1988).
- [3] M.B. Gavelle, A. Le Yaouanc, L. Oliver, O. Pène, J.C. Raynal, and S. Sood, Phys. Lett. **82B**, 431 (1979).
- [4] O.W. Greenberg and H. Lipkin, Nucl. Phys. **A370**, 349 (1981); H.J. Lipkin, Phys. Lett. **113B**, 490 (1982); K.F. Liu, *ibid.* **131B**, 195 (1983); A.O. Barut and R. Raczka, Int. J. Mod. Phys. A **2**, 265 (1987).
- [5] Th. Pfenninger and A. Faessler, Nucl. Phys. **A484**, 476

- (1988).
- [6] M. Harvey and J. LeTourneux, Nucl. Phys. **A424**, 419 (1984); M. Harvey, J. LeTourneux, and B. Lorazo, *ibid.* **A424**, 428 (1984).
- [7] R. Girard and J. LeTourneux, Report No. UdeM-LPN-TH-74, 1992.
- [8] H. Feshbach, Ann. Phys. (N.Y.) **5**, 357 (1958); **19**, 287 (1962).
- [9] See, for example, L.D. Landau and E.M. Lifshitz, *Quantum Mechanics* (Pergamon, London, 1959).